



Published in final edited form as:

*J Nat Prod.* 2019 September 27; 82(9): 2400–2408. doi:10.1021/acs.jnatprod.8b00962.

## Studying Mass Balance and the Stability of (*Z*)-Ligustilide from *Angelica sinensis* Helps to Bridge a Botanical Instability-Bioactivity Chasm

Kemal Duric<sup>†,‡</sup>, Yang Liu<sup>†</sup>, Shao-Nong Chen<sup>†,§</sup>, David C. Lankin<sup>†,§</sup>, Dejan Nikolic<sup>†</sup>, James B. McAlpine<sup>†,§</sup>, J. Brent Friesen<sup>§,⊥</sup>, Guido F. Pauli<sup>†,§</sup>

<sup>†</sup>UIC/NIH Botanical Center, Program for Collaborative Research in the Pharmaceutical Sciences (PCRPS) and Department of Pharmaceutical Sciences, College of Pharmacy, University of Illinois at Chicago, Chicago, Illinois 60612, United States

<sup>‡</sup>Department of Pharmacognosy, Faculty of Pharmacy, University of Sarajevo, Zmaja od Bosne 8, 71000 Sarajevo, Bosnia and Herzegovina

<sup>§</sup>Center for Natural Product Technologies, Program for Collaborative Research in the Pharmaceutical Sciences (PCRPS) and Department of Pharmaceutical Sciences, College of Pharmacy, University of Illinois at Chicago, Chicago, Illinois 60612, United States

<sup>⊥</sup>Department of Physical Sciences, Rosary College of Arts and Sciences, Dominican University, River Forest, Illinois 60305, United States

### Abstract

Numerous reports assigning (*Z*)-ligustilide (**1**) the role of a major bioactive principle in Apiaceae botanicals are called into question by the recurrent demonstrations of **1** being an unstable, rapidly degrading compound, ultimately leading to dynamic Residual Complexity. While *Angelica sinensis* is recognized for its therapeutic value in (peri-)menopausal symptom management, its purported active principle, ligustilide, represents a typical example for the instability-bioactivity chasm of botanicals. To help bridge the gap, this study used both the essential oil and purified **1** obtained from *A. sinensis* to investigate the factors that influence the chemical transformation of **1**, the products formed, and the rationale for monitoring **1** in natural product preparations.

Countercurrent separation was used to purify **1** from a supercritical fluid extract of *A. sinensis*, achieving 93.4% purity in a single step. Subsequent purification by preparative HPLC afforded **1** with a 98.0% purity. Providing a mass balance setting, we monitored chemical changes occurring to highly purified **1** under various conditions and at different time points, in sealed NMR tubes by

<sup>§</sup>Corresponding Author Tel: (312) 355-1949. Fax: (312) 355-2693. gfp@uic.edu.

#### ASSOCIATED CONTENT

##### Supporting Information

The Supporting Information is available free of charge at the [ACS Publications website](#) at DOI: pending ACS action. It includes NMR and qNMR spectra with quantitation calculations, chromatographic information such as for preparative purification and knock-out extract production, time course studies, and LC-MS data.

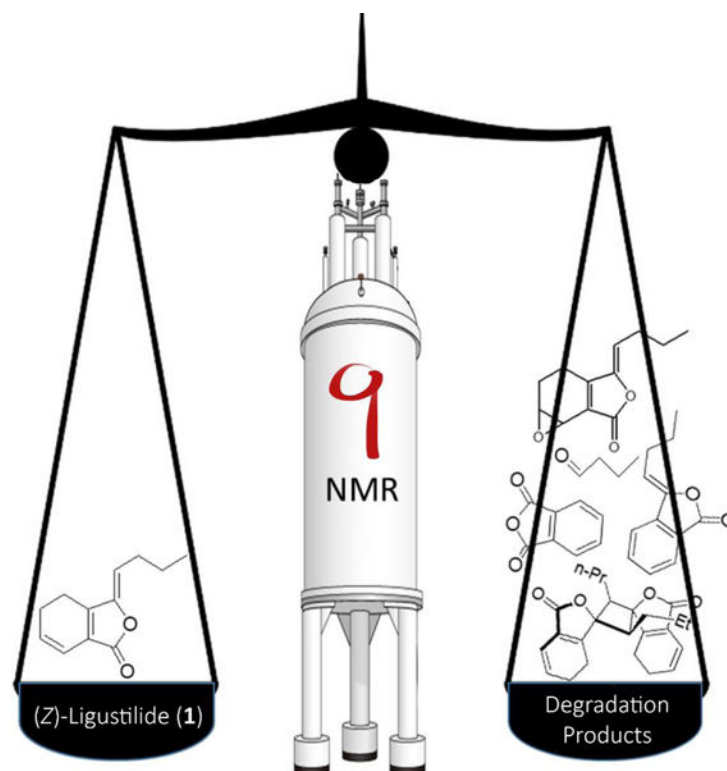
The original NMR data (FIDs) are made available at [DOI:10.7910/DVN/ONFHDT](https://doi.org/10.7910/DVN/ONFHDT).

The authors declare no competing financial interest.

This article is #32 in the series of publications on Residual Complexity.

quantitative  $^1\text{H}$  NMR (qHNMR). The non-destructive nature of NMR enabled a comprehensive assessment of degradation products. Moreover, in being a mole-based determination, the total intensity (integral) of all NMR signals intrinsically represent the theoretical mass balance within the sample solution. The results demonstrated that **1** is most stable while within the original plant material. Exposure to light had a profound impact on the chemical transformation of **1** leading to the formation of ligustilide dimers and trimers, as verified by both NMR and LC-HRMS studies. Moreover, the results shown for **1**, augmented by other recent outcomes, have serious implications for the meaningful biological evaluation of NPs which exhibit instability/reactivity, while having a plethora of “promising” bioactivities reported in the literature and being frequently associated with unsubstantiated health claims.

## Graphical Abstract



Phthalides such as the prototypical dihydro-phthalide, (*Z*)-ligustilide (**1**), are designated frequently as marker compounds of medicinal plants from the most prominent genera of the Apiaceae family, including *Ligusticum* and *Angelica*.<sup>1,2</sup> Typically, depending on the phytochemical depth of the studies, **1** and its congeners are broadly associated with observed and/or ethnobotanically documented bioactivities of the plants and their preparations. Representing an exemplary case, the predominant use of *Angelica sinensis* (Oliv.) Diels for the treatment of irregular menstrual cycles and premenstrual syndrome<sup>3,4</sup> is also linked to **1**. Studies of *A. sinensis* preparations and its metabolites cover a host of pharmacological endpoints: anti-inflammatory effects,<sup>5,6</sup> improvement of cognitive function,<sup>7</sup> alleviation of brain damage,<sup>8</sup> inhibition of tumor necrosis factor in some cell lines,<sup>9</sup> nephron-protective

effects,<sup>10</sup> and neuroprotective activities.<sup>11</sup> Interestingly, most studies primarily associate observed bioactivities with the presence and abundance of **1**, and sometimes its derivatives.

Reductionist interpretations designating **1** the role of a major bioactive principle are strikingly abundant in the literature. These assignments are called into question by the recurrent assertion that **1** is an inherently unstable and rapidly degrading compound. Representing a particularly complicated form of dynamic Residual Complexity (RC; known to entail dynamic and static forms; see [go.uic.edu/residualcomplexity](http://go.uic.edu/residualcomplexity)), the decomposition of **1** leads to a wealth of degradation products that form spontaneously and often rapidly, depending on the physical conditions of the reaction environment. Recent reports have begun to take the unstable nature of **1** into account when performing interdisciplinary pharmacological studies.<sup>12, 13</sup> However, numerous questions remain with regard to bridging the chasm between chemical instability and the biological effects of *A. sinensis* and other botanicals.

The presence of a chemically active dihydrobenzene moiety explains the tendency of **1** to undergo chemical degradation through the oxidation (including redox), cycloaddition, and isomerization reactions shown in Figure 1.<sup>14</sup> Photochemical initiated reactions of the three olefinic functions of **1** lead to the formation of cyclodimers, creating a host of structural possibilities of closely related but spatially very different molecules, especially considering the stereochemical possibilities for photocyclization.<sup>15</sup> The unstable nature of *Z*-ligustilide (**1**) makes preparation and preservation of dietary supplements containing **1** a challenge. Although a considerable number of degradation products have been isolated and structurally elucidated,<sup>12,16</sup> details of the degradation behavior of **1** are still unclear. Studies exploring the degradation mechanisms have been conducted with dried and purified **1**.<sup>12</sup> Other studies have involved the use of solutions of **1** in a variety of solvents,<sup>17</sup> or mixed with antioxidants and/or stabilizing agents,<sup>18</sup> at different temperatures, pH values, and under various light-mediated conditions.

While a considerable number of degradation pathways have been elucidated,<sup>12,19,20</sup> studies have not fully addressed one fundamental tenet of chemistry: the principle of mass balance. It applies universally, and accordingly must have a profound impact on the biological assessment and standardization of *A. sinensis* extracts and other products containing **1**. To fill this knowledge gap, a mass balance study on **1** using quantitative <sup>1</sup>H NMR (qHNMR) in sealed NMR tubes was selected as the central theme of the present study. Flame-sealed NMR tubes created an inherently mass balanced environment where matter can neither enter nor exit the sample under investigation. One intrinsic advantage of the mass balance-qHNMR approach was that the quantitative loss of **1** was determined readily for any length of time without errors introduced by sampling procedures. In addition, the mass balance-qHNMR approach had the potential to provide insight into the structural nature of the identified degradation products as they were observed in situ without the perturbations of sampling and chromatography procedures. Moreover, the application of mass balance created the opportunity to quantitatively correlate the loss of (in this case) **1** with the build-up of degradation products. Theoretically, the loss of **1** may be reasonably reconciled to the amount of all detected and quantified degradants with the achievement of full mass balance. The use of both an external calibrant and an internal reference compound reinforced the

quantitative nature of the experimental design. This study, therefore, provided the basis for a quality control mechanism for applied analytical methods, demonstrating that major degradation products were adequately detected, accounted for quantitatively, and quantified without interference by the main marker analyte.

This study investigated the influence of temperature, light, and oxygen vs. Ar (inert atmosphere) on the chemical transformation of **1**. The study also evaluated the stability of **1** in the crude *A. sinensis* plant material. The stability of **1** in the essential oil and as a purified compound dissolved in deuteriochloroform (CDCl<sub>3</sub>), was monitored by employing a mass balance-qHNMR approach.

## RESULTS AND DISCUSSION

The present study investigated the stability of *Z*-ligustilide (**1**) in plant material, in a supercritical fluid extraction (SFE) extract, representing *A. sinensis* essential oil, and as a purified compound dissolved in the widely used (NMR) solvent, deuteriochloroform.

### Extraction of **1** from *A. sinensis* Roots.

The majority of phthalides, **1** included, are relatively non-polar components of the essential oils in their plant of origin. Extraction techniques that typically might be used include extraction with lipophilic organic solvent, steam distillation, and supercritical fluid extraction (SFE). This work employed solvent modified CO<sub>2</sub> SFE of *A. sinensis* dry roots. Table 1 compares the neat and solvent modified methods. The yield of the yellowish essential oil was 1.5% w/w (essential oil/dry plant material).

### Quantitation of **1** with qHNMR.

Quantitative analyses of **1** were made by qHNMR using DMSO<sub>2</sub> as an external calibrant (EC).<sup>21</sup> Although many regions of the <sup>1</sup>H NMR spectra were complex and with overlapped signals, quantification of **1** could be performed using the characteristic signal at δ 6.286 (1H, H-7).<sup>22</sup> The average % w/w of ligustilide in three SFE essential oil samples was 14.8%. Section S2 of the Supporting Information provides NMR spectra of essential oil and a detailed method with the formula used for the absolute quantification method. Previous work with neat CO<sub>2</sub> SFE extraction indicated a 10% w/w content of **1** in the essential oil.<sup>20</sup>

### Stability of **1** in *A. sinensis* Plant Material.

Two samples of the same *A. sinensis* root specimen were created. The first sample was extracted at the beginning of the year and the percentage of **1** in the SFE essential oil was determined by the qHNMR method. The second sample was stored one year at room temperature, in the absence of light, and in a dry location extracted under the same conditions used for the first sample. The percentage of **1** in this sample was determined under the same experimental conditions as employed on the first sample. The content of **1** in both SFE extracts was nearly identical at 14.8% w/dry weight. This indicated that the intact cellular milieu of the plant materials protected **1** from both loss and degradation. Histologically, **1** is part of the essential oil in *A. sinensis* roots, where it is located in oil cavities and tubules situated within the cellular parenchyma. This environment apparently

minimized the influence of factors that may have led to the loss and degradation of **1**. This result indicated that being stored in the form of raw material may preserve the plant metabolome.

### Stability of **1** in *A. sinensis* SFE Essential Oil.

In order to calculate the stability of **1** in the essential oil, three different SFE essential oil samples were created from the same extract. Each sample contained the SFE essential oil (20 mg) dissolved in CDCl<sub>3</sub> (600 μL). The content of **1** in the SFE essential oil extract was monitored over a four-month period (from November to March). The first NMR tube (sample A1) was sealed with Parafilm<sup>®</sup> and stored in the dark at -20 °C. The second sample (A2) was flame-sealed and maintained at room temperature exposed to direct full-daylight, all day, for the duration of the experiment (January - April). The third sample (A3) was degassed with argon, flame sealed, and maintained in the dark at -20 °C. During the four-month period, qHNMR analyses<sup>23,24</sup> were conducted at the following time points: days 1, 3, 5, 7, 11, 18, 25, 34, 74, and 114, as shown in Figure 2. Samples kept in the dark at -20°C exhibited remarkable stability of **1** in the SFE essential oil regardless of the presence or absence of air. On day 114, the loss of **1** in A1 was 10.1% w/w, whereas sample A3 (degassed with Ar) lost 14.8% w/w of **1**. The reason for the difference in percentages may have been residual evaporation from the NMR tube despite careful sealing with a cap plus flexible film. All NMR tubes were flame-sealed for the subsequent experiments in order to create consistent mass balanced conditions. In the presence of direct full-daylight, sample A2 lost 45.1% w/w of **1** after 114 days. This made it evident that light and/or temperature foster the instability of **1**.

### HSCCC Purification of **1**.

The isolation of purified **1** from the SFE essential oil was achieved by high-speed countercurrent chromatography (HSCCC).<sup>25-28</sup> An *n*-hexane-EtOAc-MeOH-water (9:1:9:1, v/v) solvent system exhibited optimum resolution characteristics with a partition coefficient (*K* value) of 2.54 for **1**.<sup>29</sup> Fractions collected from 672 to 804 min contained purified **1**. Using normal-phase TLC, with the upper phase of *n*-hexane-EtOAc-MeOH-water (9:1:9:1, v/v) as the mobile phase, a single zone at *R<sub>f</sub>* value of 0.45 gave a blue-gray color spot under UV light at 356 nm, which was readily visualized with vanillin-H<sub>2</sub>SO<sub>4</sub> reagent (S3, Supporting Information). In addition to TLC, fractions were analyzed for purity with the qHNMR 100% method<sup>22,30</sup> prior to being re-combined to give purified **1**.

The quantity of **1** in the combined fraction was determined by qHNMR with DMSO<sub>2</sub> as the EC. The yield of **1** from 150 mg of SFuE essential oil separated by HSCCC in a single step was 18.7 mg (12.4% w/w), and the qHNMR purity was 93.4% w/w (S4, Supporting Information). Considering that the content of ligustilide in the original SFE essential oil extract was 14.8% w/w, the overall recovery of the HSCCC process was 78.5% w/w, which is unexpected for an unstable compound. Section S4. of the Supporting Information provides NMR spectra of both purified **1** and the combined remaining fractions (**1** knockout extract) of *A. sinensis* SFE essential oil obtained by HSCCC fractionation. The 93.4% w/w purity was sufficient for studying the general influence of environmental factors in the following experiment.

### The Influence of Light on the Stability of Purified **1**.

In order to study the influence of light, purified **1** (5.4 mg, HSCCC purity, 93.4% w/w) was dissolved in 1500  $\mu\text{L}$  of  $\text{CDCl}_3$  and the solution distributed equally into three NMR tubes, flame-sealed, and kept at room temperature. The first NMR tube (B1) was exposed to direct full-daylight, all day, for the duration of the experiment, the second (B2) was kept in the dark, and the third (B3) was exposed continuously to UV light (260 nm). Figure 3 shows that the B1 did not show any detectable **1** after 15 days. On the other hand, minimal degradation of **1** occurred in B2 during the same time period. In the case of B3, exposed to 260 nm UV light, the degradation of **1** closely followed B1 for six days. These results showed a very strong influence of light on the stability of **1** under mass balance conditions.

The possible degradation of chloroform and stability of residual  $\text{CHCl}_3$  as an internal reference over the time course of the experiment was monitored as well (S9, Supporting Information). In conclusion, no light-mediated effects on the solvent occurred under these conditions as the residual solvent signal remained unchanged.

### Mass Balance Characterization of Degradation Products.

In order to enhance the rigor of the third mass balance study, the combined HSCCC fractions were subjected to preparative HPLC (see S6, Supporting Information), which increased the purity of **1** to 98.0%, determined by qHNMR.

In order to investigate the nature of the degradation products by mass balance-qHNMR, two NMR tubes were prepared. Sample C1 contained 1.8 mg of **1** (98.0% qHNMR purity) in 500  $\mu\text{L}$   $\text{CDCl}_3$  in a flame-sealed NMR tube. An identical sample of **1** (C2) was prepared and degassed with Ar to exclude air/ $\text{O}_2$  before flame-sealing. Both samples were kept in the dark at  $-20\text{ }^\circ\text{C}$  for 30 days, after which the samples were maintained at ambient temperature exposed to direct full-daylight, all day, for the next ten days.

Flame-sealing prevented evaporation of solvent and volatile degradation products. According to the law of conservation of mass, the mass of the products in a chemical reaction must equal the mass of the reactants. Flame-sealed NMR tubes, utilized in this investigation, provided an enclosed system (matter cannot enter or exit), which represents the basic prerequisites for mass balance calculations. A control test weight was performed in order to exclude the possibility that the tubes were not properly sealed, which would lead to the loss of the volatile components. The sealed tubes were weighed on the first and last day of the mass balance experiment. No change in weight was noted (Sample C1: day 1 weight = 3100.92 mg and day 41 weight = 3100.89 mg. Sample C2 day 1 weight = 3322.20 mg and day 41 weight = 3322.28 mg), validating the true mass balance conditions, which were key prerequisites of the mass balance-qHNMR approach.

The dynamics of the chemistry in the samples under mass balance conditions were analyzed by qHNMR on days 1, 3, 14, 30, and 41. LC-MS analyses of both samples were performed on days 1 and 41. The collective interpretation of the qHNMR and MS results led to the identification and quantification of **1** and four degradation products that contributed towards understanding the mass balance. Figure 4 shows the structures of **1** and the identified degradation products: *endo-Z,Z*-(3.8',8.3', H-7)-diligustilide (**2**); *Z*-butyridenepthalide (**3**);



phthalic acid anhydride (**4**), detected as phthalic acid (**4a**); and butyraldehyde (**5**). Each of the five compounds was quantitated by calculating the ratio of the integral value of its target signal (TS) shown in Figure 4 to that of the residual CHCl<sub>3</sub> solvent (RS) in the sample (TS/RS). This was possible because the integral value of the residual solvent (CHCl<sub>3</sub>) was constant during the time course of the degradation of (*Z*)-ligustilide (**1**) shown in S7. Supporting Information.

During the first 30 days, when the C1 sample was kept in the dark at -20 °C, degradation of **1** was observed: the initial TS/RS of 8.43 decreased by 21.5 % to 6.62 as shown in Figure 5 and Figure S11, Supporting Information. A consistent increase of the degradation products **2**, **3**, and **5** was observed during this time. After 30 days, C1 was kept at room temperature, full-daylight, all day, from February to March. As a result, the total degradation of **1** was observed within the next ten days (Figure 5). All four degradation products increased from days 30 to 41. However, there was a dramatic increase in the quantity of the dimer **2** between days 30 and 41 (Supporting Information S6), with a TS/RS of 3.81 (45.2%). Understandably, the photochemically induced dimerization was most affected by the change in conditions. Moreover, according to the upfield region of the <sup>1</sup>H NMR spectrum (S7. Supporting Information), it was evident that other aliphatic degradation products were produced. Due to extensive spectral overlap, however, it was difficult to identify a single compound. This observation helps to explain the overall decrease of TS/RS over the duration of the experiment. Other degradation products were formed but were not identifiable nor quantifiable by qHNMR.

The LC-MS and qHNMR data, when taken initially and after 41 days, were compared. A standard dereplication approach used in mass spectrometry-based metabolomic studies, beginning with the determination of elemental composition by accurate mass measurement, followed by the acquisition of product ion tandem mass spectra, was employed. On day 1, the LC-MS chromatogram showed two main components: one with protonated molecule at *m/z* 191, and another with the protonated molecule at *m/z* 188. Comparison of the NMR data with the LC-MS data showed the presence of **1** and *Z*-butylidenephthalide (**3**). After 41 days, the LC-MS chromatograms indicated the presence of oxygenated products (*m/z* 207) and dimers at *m/z* 381. Interestingly, multiple peaks eluting between 26 and 30 min with protonated molecules at *m/z* 571 were also observed. The elemental composition of these ions, C<sub>36</sub>H<sub>42</sub>O<sub>6</sub>, suggested that they might be trimers of ligustilide (S7, Supporting Information).<sup>31</sup> Further investigations will be required to clarify the structures and stereochemistry of trimer formation. The presence of trimers detected by LC-MS but not quantifiable by qHNMR also helps explain the overall decrease in TR/RS from days 30 to 41. The comparison between LC-MS and qHNMR results were largely qualitative, and not quantitative, because the purified reference compounds required to calculate LC-MS response factors were not available for some analytes.

Further consideration of overall loss of qHNMR integral value led to proposing the formation of volatile degradation products (such as **5**) that may have entered the gas phase of the sample and, thereby, escaped detection in the liquid by the NMR probe. The volatile degradation products in sample C1 may be due to the formation of smaller (volatile)

molecules, even H<sub>2</sub>, via oxidative cleavage reactions. Future studies could employ headspace GC-MS for the qualitative and quantitative determination of volatile compounds.

The situation was different for the sample C2 under Ar. For the first three days (−20 °C and dark storage), **1** showed good stability, with the TS/RS changing only slightly from 13.4 to 13.2. When comparing sample C1 with C2 during the first 30 days, the change in TS/RS of **1** was lower for C2 (degassed with Ar) when being exposed to otherwise identical storage conditions. Apparently, the presence of oxygen in C1 led to some degradation. Degassing the sample with Ar helped to slow down oxidation but did not prevent it entirely. The amounts of **2**, **3**, and **5** increased steadily from days 1 to 30. However, the presence of **4** was not detected during that time.

After being exposed to sunlight at room temperature, **1** in sample C2 decomposed rapidly within 10 days. After 41 days the TS/RS of **1** was only 0.2 (Figure 5). Similar to sample C1, the bulk of **1** apparently underwent degradation to the photodimer **2**, showing a TS/RS of 13.05 at day 41 (S9, Supporting Information). Balancing the initial TS/RS value of **1** (13.39) with the four main degradation products **2** (13.05), **3** (0.33), **4** (0.04) and **5** (0.30) after 41 days, demonstrated a near 100% mass balance of the degradation pathway under an Ar atmosphere. The quantity of **1** and its degradation products over the course of the experiment is given in S11. Supporting Information.

Qualitatively, the LC-MS profile of sample C2 after 41 days was very similar to that of sample C1. In both samples, formation of **2**, **3**, **4**, and **5** was evident, albeit at different ratios. In this work, the fundamental approach in determining mass balance was to quantitate the main degradation products. The measured loss in the initial amount of **1** was then reconciled with the total amount of degradation products. The second value was converted to the corresponding percentage of degraded **1** by means of the ratio of the quantity of new formed compound to that of residual CHCl<sub>3</sub> (TS/RS), which had to be constant due to the mass balance conditions.

From the quantitative perspective, it was noted that, under the chosen conditions (presence vs. absence of O<sub>2</sub> after Ar degassing in C1 vs. C2, respectively), the total integral of the NMR solutions on day 1 differed from those on day 41. While their weight was constant until day 41, the C1 sample showed only 58% of the initial total <sup>1</sup>H integral, whereas 98.0% of the initial total integral could be accounted for in sample C2 after the same period. Apparently, the variety and quantity of non-quantifiable degradation products in sample C1 was greater than in sample C2.

The comparison of all four of the experiments brought two important aspects to light. The purity of **1** was inversely proportional to its propensity to be chemically transformed in the presence of light. Experiments with 98.2% w/w samples showed that the predominant product of degradation in the presence of light was the dimer **2**. Similarly, the purity of **1** was inversely proportional to its propensity to be chemically transformed in the presence of oxygen (compare samples A1 and C1), although the overall effect was much less than light. The effect of temperature was not tested directly with the experiments in this study. The purity of **1** was only one aspect of the comparison. The other aspect was the identity and



characteristics of the “impurities.” In the form of dried roots, **1** may be described as “crude” or “low-purity” but the immediate environment of **1** had a stabilizing effect. In the form of a SFE essential oil, the accompanying impurities (other non-polar compounds that comprised the essential oil) also had a stabilizing effect even when the mixture was diluted in a CDCl<sub>3</sub> solution. When accompanying “impurities” are largely removed, the stability of **1** was affected significantly.

### Conclusions Regarding qHNMR Methodology.

In addition to shedding light on the stability of **1** in different forms (dried plant material, SFE essential oil, 93.4% w/w purity **1**, and 98.2% w/w purity **1**), the series of experiments also revealed how the method analysis may affect the results. In order for qHNMR studies to be performed the sample had to be dissolved in a suitable deuterated solvent. For the dried roots, this meant that an extraction procedure was performed to obtain **1** in a desirable liquid form. For the subsequent experiments, the samples were already in a liquid form. Furthermore, one cannot assume CDCl<sub>3</sub> is entirely inert in this study. Very likely, the results would have been different if a different deuterated solvent had been used.

The advantages of qHNMR analysis for stability studies were described earlier in this report. In contrast to LC methods, a spectroscopic method could monitor the contents of a sample in a sealed glass container over a period of time. NMR spectroscopy was the obvious choice because of its sensitivity and resolving power. In addition, qNMR is fundamentally a gravimetric method that does not require response factors to convert signal integration values to moles and subsequently, grams. Finally, NMR reveals structural information as well as quantitation power. Ideally, qHNMR for this type of study requires the compounds of interest to have at least one signal that is isolated from interference by signals from other compounds in the solution.

All the hydrogen atoms in the original sample remain in the sealed tube for the duration of the experiments that were performed. However, the ability of HNMR to detect and quantify the presence of hydrogen in certain molecules may be compromised. Limits of detection and quantitation also become important in degradation studies where many low-abundance compounds may be formed as in the case of C1. The ability of qHNMR to count hydrogens is a definite advantage when working with natural products. However, there are at least two ways that hydrogens may escape detection by the NMR probe. It has already been mentioned that molecules that occupy the head space of the NMR tube are not detected. In addition, precipitated molecules will also escape detection. Fortunately, no precipitates were detected in this study.

### The Biological Potential of (Z)-Ligustilide (**1**).

The present study sheds new light on the potential implications of using the various available materials containing **1** for biological in vitro and in vivo assays: crude plant materials, crude plant extracts, enriched fractions, and **1** purified to various levels can be predicted to exhibit vastly different degrees of degradation, in terms of both abundance levels and chemical species diversity. Unless very carefully controlled, these mechanisms could disrupt not only the intra-laboratory repeatability of studies, but importantly also the global reproducibility of

studies with ligustilide-type botanicals. From the general perspective of elucidating bioactive markers in botanical products, it should finally be noted that essential oils and related lipophilic phytoconstituents have a tendency to be unstable, especially when removed from the cellular context of their producing organism.<sup>32</sup>

**About Reproducibility.**—Moreover, the significant instability and elucidated mass balance degradation patterns of (**1**) can serve to explain some of the illogicality and difficulty in the reproducibility and repeatability of results when supposedly identical experiments allegedly use the same **1**-containing materials. As **1** has been the focus of a large number of studies that report positive outcomes and numerous targets for potential therapeutic use, it is even more important that future studies consider the unstable nature of **1** in their study design. This includes both the characterization of **1** in the intervention materials (purity, Residual Complexity, demonstration of its static nature, and/or elucidation of its dynamic Residual Complexity) as well as its fate in the biological system (dynamic Residual Complexity). From a general point-of-view, the results presented here align well with a very recent report by Sheng et al. on the direct and metal-catalyzed photochemical dimerization of (*Z*)-ligustilide (**1**).<sup>33</sup> A host of dimers previously from Apiaceaeous extracts was shown to form via photochemically-promoted dimerization (notably, trimers were not detected) under various photolytic conditions incl. photosensitizers, metal ions, and air.

**The IMPLICATIONS.**<sup>34</sup>—A frequent motivation for pursuing total synthesis of NPs is their “promising potential” for biological studies or future human use. Very often, organic chemists become interested in NP molecules due to reports about biological profiles that indicate potential “lead compounds”, especially when several reports point to multiple biological targets. This motivation is logical and adequately reflected when Sheng et al. state that “*Many of the phthalide-based components of such medicines have been subject to biological evaluation and so revealing they can exert a plethora of significant activities.*” However, the assumption of “significance” requires substantial re-consideration: as has been shown,<sup>34</sup> the body of the world’s literature has assigned **1** nearly every biological endpoint assessed by researchers, i.e., **1** is a designated panacea. However, based on a detailed meta analysis of the literature, we have also demonstrated that **1** should rather be categorized as an Invalid/Improbable/Interfering Metabolic Panacea (IMP).<sup>34</sup> Thus, it is more plausible that the myriad of biological activities purportedly exhibited by **1** are either not meaningful or not directly connected to **1** but to other chemical species. To reproduce these reported bioactivities requires a higher degree of scrutiny for their (re-)assessment. The present findings, augmented by the findings by Sheng et al., support the need for a more rigorous approach.

**About Residual Complexity.**—Based on the evidence produced in our and the laboratories of others, **1** can be considered an exemplary case of both (dynamic) Residual Complexity (see [go.uic.edu/residualcomplexity](http://go.uic.edu/residualcomplexity)) and an IMP that tends to mislead research efforts.<sup>34</sup> The compound is highly unstable under certain conditions, especially when purified. In contrast, it is surprisingly stable in the crude plant material, which has implications for the use of medicinal plants and dietary supplements. However, from a chemical perspective, it is now clear that **1** undergoes self-degradation in an isolated,

“neutral” environment such as sealed NMR tubes used in the present study. At the same time, as shown by Sheng et al.,<sup>33</sup> the compound undergoes photo-induced self- and metal-mediated dimerization. Considering that metals are present in most biological (test) systems, this also has implications on the dynamic Residual Complexity of bioassays. As shown here, oligomerization can even occur sealed solutions. Collectively, these findings strongly imply that dynamic Residual Complexity of **1** is the main, if not the sole source of biological activity of preparations of **1**, whether they utilize the purified compound, a plant extract or enriched fractions containing **1**.

**About Perspectives.**—One plausible hypothesis for future chemical and biological studies of (*Z*)-ligustilide (**1**) and its preparation would be that mostly, or even only, the derivatives and degradation products generated from **1** that produce the observed biological effects. This means that monitoring the reactivity, instability, and degradation chemistry is key to understanding the biological profiles of **1** and any botanical products containing it or derived from it. Notably, this concept potentially extends to other NPs, especially to those with known instability/reactivity, and reported to have a plethora of biological activities (“panaceas”), such as curcumin.<sup>35,36</sup> The mass balance approach applied in the present study of **1** is a useful tool for studying these types of botanical markers from other plants and, thereby, advance botanical standardization protocols via consideration of the evident impact of dynamic Residual Complexity.

## DEDICATION

Dedicated to Dr. Jon Clardy, Harvard University, Cambridge (MA), for his pioneering work on bioactive natural products.

## EXPERIMENTAL SECTION

### Plant Material.

Angelicae Radix (*Angelica sinensis*, Apiaceae, BC440) was purchased from Nam Bac Hang, a local store in Chinatown, Chicago, IL, USA. The plant roots were harvested after three year growth in Gansu, Peoples Republic of China. The plant material was identified through a series of comparative macroscopic, organoleptic, and TLC analyses against a genuine plant voucher (927–200110, National Institute for Food and Drug Control, Peoples Republic of China) deposited at the UIC/NIH Center for Botanical Dietary Supplements Research, Chicago, IL. It also was confirmed with a genetic approach using DNA barcoding (see Supporting Information). The plant material was stored in a dry location in the absence of light at room temperature.

### Supercritical Fluid Extraction (SFE).

Production of the SFE essential oil used a Speed SFE instrument, model 7070 (Applied Separation Inc. Allentown, PA, USA), consisting of a column oven, air pressure regulator, and a 195 mm × 75 mm i.d. stainless steel column, connected to a NESLAB RTE 7 refrigerated bath (Thermo Electron Corporation, Waltham, MA, USA). Compressed air and CO<sub>2</sub> were purchased from Airgas Inc., Radnor, PA, USA. The extraction column was filled

with powdered plant material (69 g). Glass wool was added at each end of the column. As modifier, methanol was added at a concentration of 5% to the part of column where the CO<sub>2</sub> entered into the column. The extraction temperature was set to 50 °C. Extraction was performed at 250 psi, with a static extract time of 30 min and at a flow rate of 0.5 mL/min, four times for each sample. The SFE extract was then collected in glass vials and stored at -20 °C.

### High-speed Countercurrent Chromatography (HSCCC).

These separations were performed on a high-speed countercurrent chromatograph (model CCC-1000 Pharma Tech Research Co., Baltimore, MD, USA) consisting of a self-balancing three-coil centrifuge with a total volume of 320 mL and a 10 mL sample loop. The system was attached to digital single piston pump (Lab Alliance series II) for solvent delivery and a fraction collector (LKB Bromma 2111 Multirac, Sweden). The *n*-hexane-ethyl acetate-methanol-water (9:1:9:1, v/v) solvent system was used with the following conditions: 800 rpm rotation speed, 1.0 mL/min flow rate, 89% stationary phase retention volume ratio (*S<sub>f</sub>* value), and 90 psi system pressure after equilibration. Fractions were collected in 12 min intervals.

### Thin-Layer Chromatography (TLC).

In order to monitor **1** and its congeners in the HSCCC fractions, TLC was performed using pre-coated silica gel 60 plates (ALUGRAM SIL G/UV<sub>254</sub>, Macherey-Nagel Inc, PA, USA). The upper phase of *n*-hexane-EtOAc-MeOH-water (9:1:9:1, v/v) solvent system was used as the eluent. Detection of **1** was achieved by observation under UV<sub>354/254</sub>, and by spraying with vanillin H<sub>2</sub>SO<sub>4</sub> reagent (0.8 g of vanillin dissolved in 100 mL of EtOH, with 2 mL of concentrated H<sub>2</sub>SO<sub>4</sub> added), and heating with a heat gun until full color development.

### Preparative HPLC.

This was conducted on a Waters 600 system coupled with a photodiode array (PDA) detector, a Waters 717 plus auto-sampler, and Millennium32 Chromatography Manager (Waters Corporation), using a Watrex GROMSil 120 ODS-4 HE column (5 μm, 20 × 300 mm) at a flow rate 1.6 mL/min. The binary mobile phase consisted of a water (solvent A) to acetonitrile (solvent B) gradient as follows 87% A isocratically from 0 to 10 min, 50% A at 35 min, 5% A isocratically from 36 to 38 min, and 87% A at 40 min, with a 2-min post-run for column reconditioning. The detection wavelength was set at 254 nm, and the fractions were collected and analyzed by qHNMR (see S6 Supporting Information).

### LC-MS Analysis.

Reversed-phase separations were carried out on a YMC AQ column 2 × 100 mm column (3-μm particle size) using a mobile phase consisting of 0.1% formic acid (solvent A) and 95% CH<sub>3</sub>CN (solvent B) and the following gradient program: 30–90% B over 30 min. The flow rate was 0.2 mL/min, and the column was kept at a constant 30 °C. Typically, 2–5 μL of a 0.2–0.3 mg/mL test solutions were injected for LC–MS analysis. Mass spectrometric data were acquired using a Waters (Milford, MA, USA) SYNAPT hybrid quadrupole/time-of-flight mass spectrometer with positive-ion electrospray. Data were acquired at 10,000

FWHM resolution using Leu-enkephalin as the lock mass, which was introduced via a separate sprayer. Peak centroiding was carried out during data acquisition using the extended dynamic range option available in the MassLynx software.

### NMR Analysis.

Samples were dissolved in 600  $\mu\text{L}$  of  $\text{CDCl}_3$  measured with an analytical syringe (Valco Instruments, Baton Rouge, LA, USA). The  $^1\text{H}$  NMR experiments on the SFE essential oil for stability evaluation and qHNMR quantitation of **1** were performed on a Bruker AVANCE 360 NMR instrument [housed in the UIC Research Resources Center (RRC)] using a 10 degree flip angle with the standard hydrogen acquisition program (zg10). Other key parameters were as follows: spectral width (SW) = 12 ppm, transmitter offset (O1P) = 6 ppm, acquisition time (AQ) = 2.77 s, receiver gain (RG) = 512, and relaxation delay (D1) = 1.0 s. For the series of experiments with a 10 degree flip angle and ca 3.77 s (AQ+D1) recycle delay, T1 effects could be ignored. This applies particularly as the same signal of **1** was evaluated and the same experimental conditions were applied during the entire experimental procedure. The  $^1\text{H}$  NMR experiments, obtained on purified **1** (98.0% purity, determined by qHNMR) and the determination of degradation products and mass balance, were performed on a Bruker Avance-800 NMR instrument [housed in the UIC Center for Structural Biology (CSB)] using the standard zg30 sequence with the following parameters: SW = 12 ppm, O1P = 4.0 ppm, AQ = 3.14 s, RG = 128, and D1 = 60 s. NMR tubes (5 mm XR-55) were obtained from Norell Inc. (Landisville, NJ, USA). Spectra were processed and analyzed using MestReNova (v.9.0.1) software (Mestrelab Research, Santiago de Compostela, Spain). A calibration curve was generated using dimethyl sulfone ( $\text{DMSO}_2$ , lot# BCBH9813V, Fluka analytical, purity = 99.73%) as the external calibrant at concentrations ranging from 0.28 to 15.13 mM. The qHNMR data were processed as follows: Lorentzian/Gaussian multiplication (EM 0.20 Hz and GB 1.00 Hz) with zero filling to 512 k prior to Fourier transformation of the FID, with baseline correction using a 5<sup>th</sup> power polynomial function, manual peak picking and integration.

### Quantitative analysis.

Absolute quantification was performed using an external calibrant. This method allows the determination of compound mass with a known structure [(*Z*)-ligustilide in the present case] in an accurately weighed sample. It involves the use of a calibrant of known exact weight and purity. When using an external calibrant, the general calculation of purity (P) is as follows:

$$P_{\text{analyte}} = \frac{I_{\text{analyte}} \times N_{\text{EC}} \times M_{\text{analyte}} \times W_{\text{EC}} \times P_{\text{EC}}}{I_{\text{EC}} \times N_{\text{analyte}} \times M_{\text{EC}} \times W_{\text{sample}}}$$

where, P is the purity of the analyte (in % w/w), I is the absolute integral value, N is the number of protons in the integrated signal, M is the molar mass, W is the gravimetric weight (in mg), and EC is the external calibrant.

## Supplementary Material

Refer to Web version on PubMed Central for supplementary material.

## ACKNOWLEDGMENTS

This research was supported by NCCAM and ODS of the NIH through grant P50 AT000155 and in part by grant U41 AT008706. The construction of the UIC Center for Structural Biology and the purchase of the 800 MHz NMR spectrometer was generously funded by grant P41 GM068944 awarded to Dr. Peter Gettins from NIGMS/NIH. We would like to acknowledge the assistance of the following individuals: Mr. Jeff Anderson for help with DNA-barcoding procedures; Dr. Seon Beom Kim for HPTLC analysis; and Dr. Hao Gao at College of Pharmacy, Jinan University, Guangzhou, Peoples Republic of China for generously sharing *Angelica* samples. Finally, K.D. gratefully acknowledges the Fulbright Foundation for providing a fellowship (Grantee ID: 68150333) that enabled him to pursue research activities at UIC Chicago, IL, USA.

## REFERENCES

- (1). Zhang X.; Feng Z-M; Yang Y-N; Jiang J-S; Zhang P-D *Bioorg. Chem* 2019, 84, 505–510. [PubMed: 30602133]
- (2). Beck JJ; Chou SC J. *Nat. Prod* 2007, 70, 891–900. [PubMed: 17477571]
- (3). Wei W; Zenq R; Gu CM; Qu Y; Huang LF J *Ethnopharmacol.* 2016, 190, 116–141. [PubMed: 27211015]
- (4). Yi L; Liang Y; Wu H; Yuan DJ *Chromatogr. A* 2009, 1216, 1991–2001.
- (5). Ma Z; Bai L. *Inflammation* 2013, 36, 294–299. [PubMed: 23007925]
- (6). Chung JW; Choi RJ; Seo EK; Nam JW; Dong MS; Shin EM; Guo LY; Kim YS *Curr. Drug. Metab* 2012, 35, 723–732.
- (7). Xin J; Zhang J; Yang Y; Deng M; Xie X. *Curr. Neurovasc. Res* 2013, 10, 304–315. [PubMed: 23937197]
- (8). Feng Z; Lu Y; Wu X; Zhao P; Li J; Bin P; Qian Z; Zhu LJ *Ethnopharmacol.* 2012, 144, 313–321.
- (9). Shi YS; Xiao L; Yin Y; Wei L. *Biomed. Pharmacother* 2015, 69, 42–46. [PubMed: 25661336]
- (10). Bunel V; Antoine MH; Nortier J; Duez P; Stevigny C. *Toxicol. in In Vitro* 2015, 29, 458–467.
- (11). Gong W; Zhou Y; Li X; Gao X; Tian J; Qin X; Du G. *Molecules.* 2016, 21, 549.
- (12). Schinkovitz A; Pro SM; Main M; Chen SN; Jaki BU; Lankin DC; Pauli GF J. *Nat. Prod* 2008, 71, 1604–1611. [PubMed: 18781813]
- (13). Zuo AH; Cheng MC; Zhuo RJ; Wang L; Xiao HB *Acta Pharm. Sin* 2013, 48, 911–916.
- (14). Karmakar R; Pahari; Mal D. *Chem. Rev* 2014, 114, 6213–6284 [PubMed: 24823231]
- (15). Quiroz-Garcia B; Figueroa R; Cogordan JA; Delgado G. *Tetrahedron Lett.* 2005, 46, 3003–3006.
- (16). Deng S. *Phytochemical Investigation of Bioactive Constituents from Angelica sinensis.* Ph.D. Dissertation, University of Illinois at Chicago, Chicago, IL, 2005.
- (17). Zhou C; Li X. *Yao Xue Xue Bao* 2001, 36, 793–795. [PubMed: 12579984]
- (18). Lu Y; Liu S; Zhao Y; Zhu L; Yu S. *Acta Pharm.* 2014, 64, 211–222. [PubMed: 24914721]
- (19). Cui F; Fenq L; Hu J. *Drug Dev. Ind. Pharm* 2006, 32, 747–755. [PubMed: 16885129]
- (20). Gödecke T; Napolitano JG; Rodriguez Brasco MF; Chen SN; Jaki BU; Lankin D; Pauli GF *Phytochem. Anal* 2013, 24, 581–597. [PubMed: 23740625]
- (21). Pauli GF; Chen SN; Simmler S; Lankin DC; Gödecke T; Jaki BU; Friesen JB; McAlpine JB; Napolitano JG J. *Med. Chem* 2014, 57, 9220–9231. [PubMed: 25295852]
- (22). Pauli GF; Gödecke T; Jaki BU; Lankin DC J. *Nat. Prod* 2012, 75, 834–851. [PubMed: 22482996]
- (23). Friesen JB; McAlpine JB; Chen SN; Pauli GF J. *Nat. Prod* 2015, 78, 1765–1796. [PubMed: 26177360]
- (24). Friesen JB; Ahmed S; Pauli GF J. *Chromatogr. A* 2015, 1377, 55–63. [PubMed: 25542704]
- (25). Pauli GF; Pro S; Friesen BJ *Nat. Prod* 2008, 71, 1489–1508.
- (26). Liu Y; Friesen JB; McAlpine JB; Pauli GF *Planta Med.* 2015, 81, 1582–1591. [PubMed: 26393937]



- (27). Simmler C; Napolitano JG; McAlpine JB; Chen SN; Pauli GF *Curr. Opin. Biotechnol* 2014, 25, 51–59. [PubMed: 24484881]
- (28). Liu Y; Friesen JB; Grzelak EM; Fan Q; Tang T; Duri K; Jaki BU; McAlpine JB; Franzblau SG; Chen SN; Pauli GF *J. Chromatogr. A* 2017, 1504, 46–54. [PubMed: 28506498]
- (29). Wells RJ; Hook JM; Al-Deen TS; Hibbert DB *J. Agric. Food Chem* 2002, 50, 3366–3374. [PubMed: 12033797]
- (30). Zou J; Chen GD; Zhao H; Huang Y; Luo X; Xu W; He RR; Hu D; Yao XS; Gao H. *Org. Lett* 2018, 20, 884–887. [PubMed: 29360378]
- (31). Turek C; Stintzing FC *Compr. Rev. Food Sci. Food Safety* 2013, 12, 40–53.
- (32). R ileanu M; Todan L; Voicescu M; Ciuculescu C; Maganu M. *Mater. Sci. Eng. C Mater. Biol. Appl* 2013, 33, 3281–3288. [PubMed: 23706211]
- (33). Sheng B; Vo Y; Lan P; Gardiner MG; Banwell MG; Sun P. *Org. Lett* 2019, in press [DOI: 10.1021/acs.orglett.9b02172].
- (34). Bisson J; McAlpine JB; Friesen JB; Chen S-N; Graham J; Pauli GF *J. Med. Chem* 2016, 59, 1671–1690. [PubMed: 26505758]
- (35). Nelson KM; Dahlin JL; Bisson J; Graham J; Pauli GF; Walters MA *J. Med. Chem* 2017, 60, 1620–1637. [PubMed: 28074653]
- (36). Friesen JB; Liu Y; Chen SN; McAlpine JB; Pauli GF *J. Nat. Prod* 2019, 82, 621–630. [PubMed: 30848909]

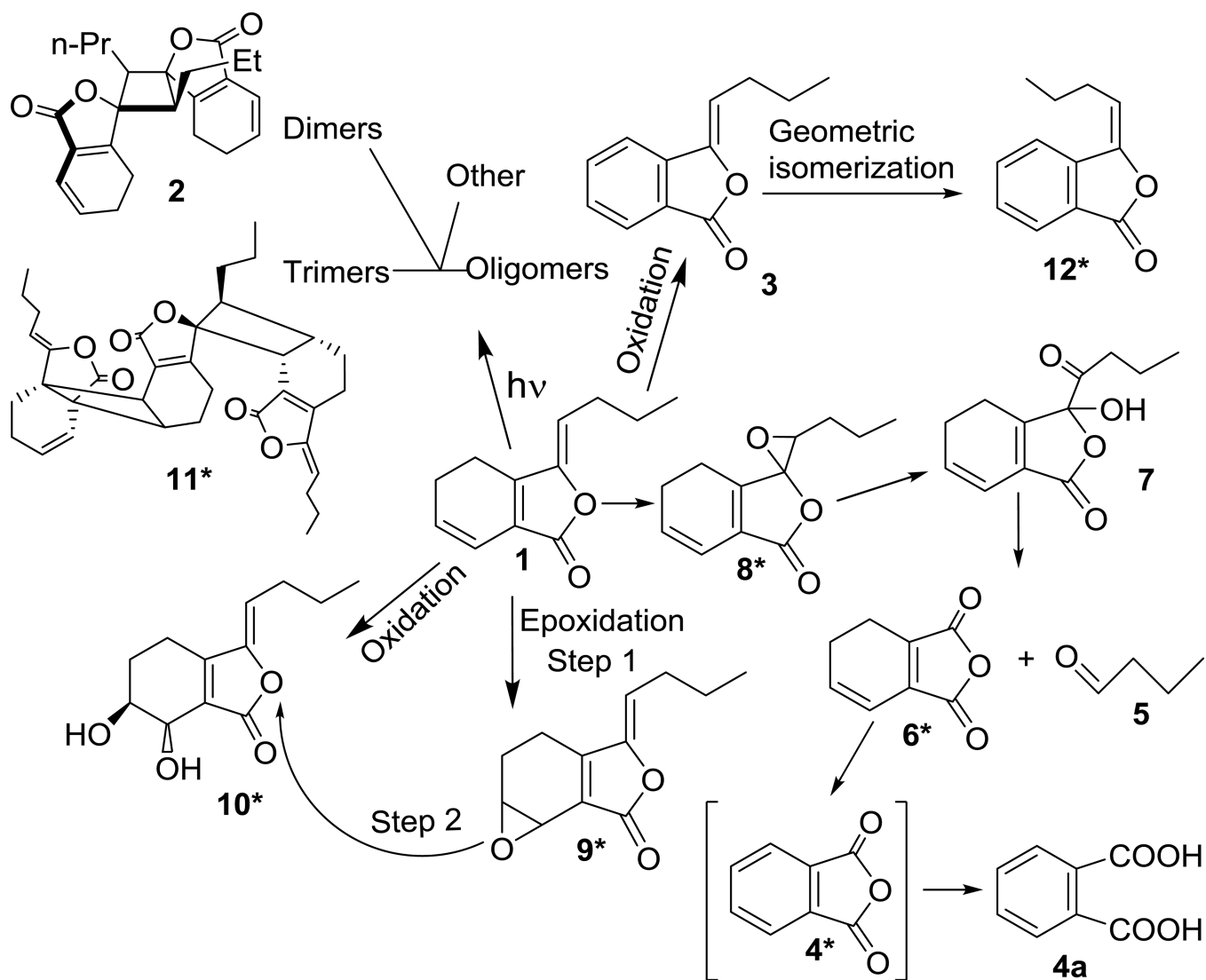


**Figure 1.** Reaction pathways from *Z*-ligustilide (1) to its main degradation products, summarizing NMR and LC-MS data from the present study, as well as from the literature (compounds marked with an asterisk \*). This involved the following degradants: *endo*-(*Z,Z*)-(3,8', 8,3',H-7)-diligustilide (2), (*Z*)-butylidenephthalide (3), phthalic acid anhydride (4<sup>12</sup>), which may be detected by NMR spectroscopy as free phthalic acid (4a), butyraldehyde (5), 4,5 dihydro-1,3-isobenzofuranon (6<sup>12</sup>), senkyunolide D (7<sup>12</sup>), 3,8-epoxyiligustilide (8<sup>12</sup>), 6,7-epoxyiligustilide (9<sup>12</sup>), senkyunolide I (10<sup>2</sup>), triligustilide A (11<sup>31</sup>), and (*E*)-butylidenephthalide (12<sup>12</sup>).

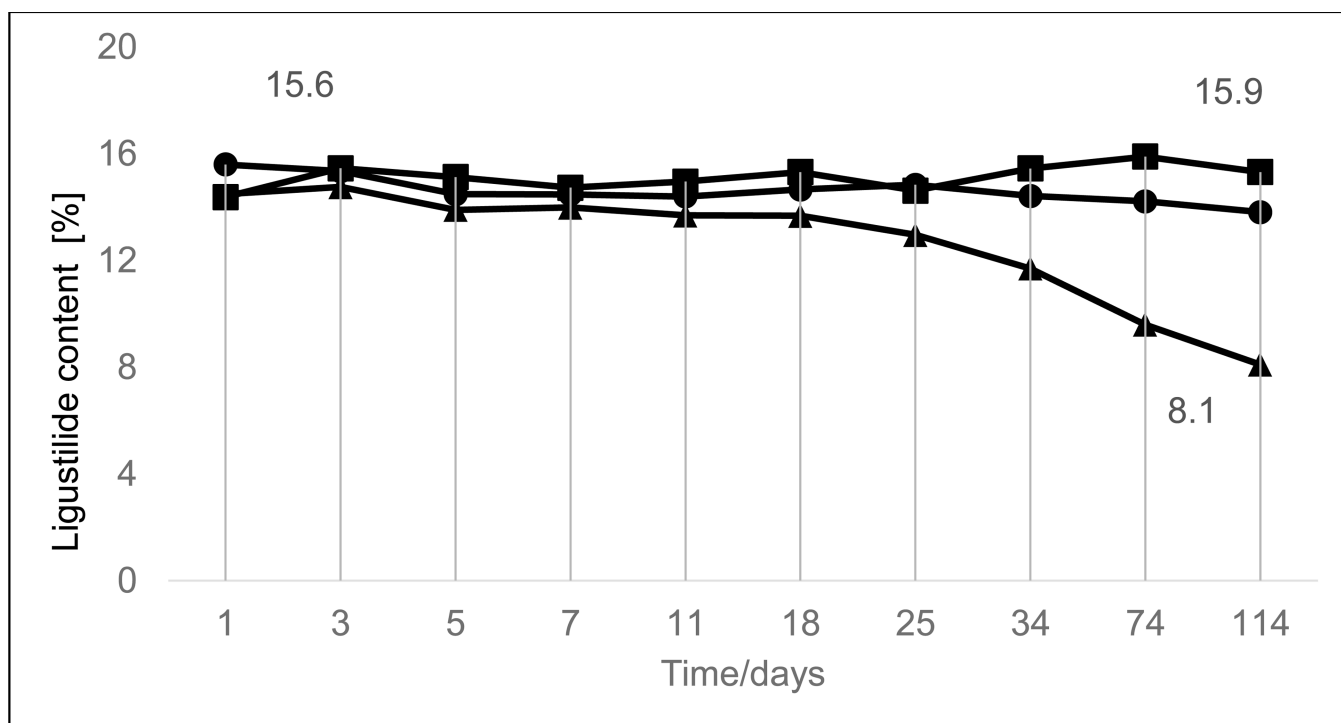


**Figure 2.**

Stability study of ligustilide (**1**) in *A. sinensis* SFE essential oil. The % content of **1** in the three NMR samples: tube sealed with Parafilm® and stored at  $-20\text{ }^{\circ}\text{C}$  [A1, ■], tube with flame sealed and stored at room temperature and in daylight [A2, ▲], and tube with Ar degassing and flame sealed, stored at  $-20\text{ }^{\circ}\text{C}$  [A3, ●]. The samples were monitored over time by qHNMR using  $\text{DMSO}_2$  as an external calibrant.

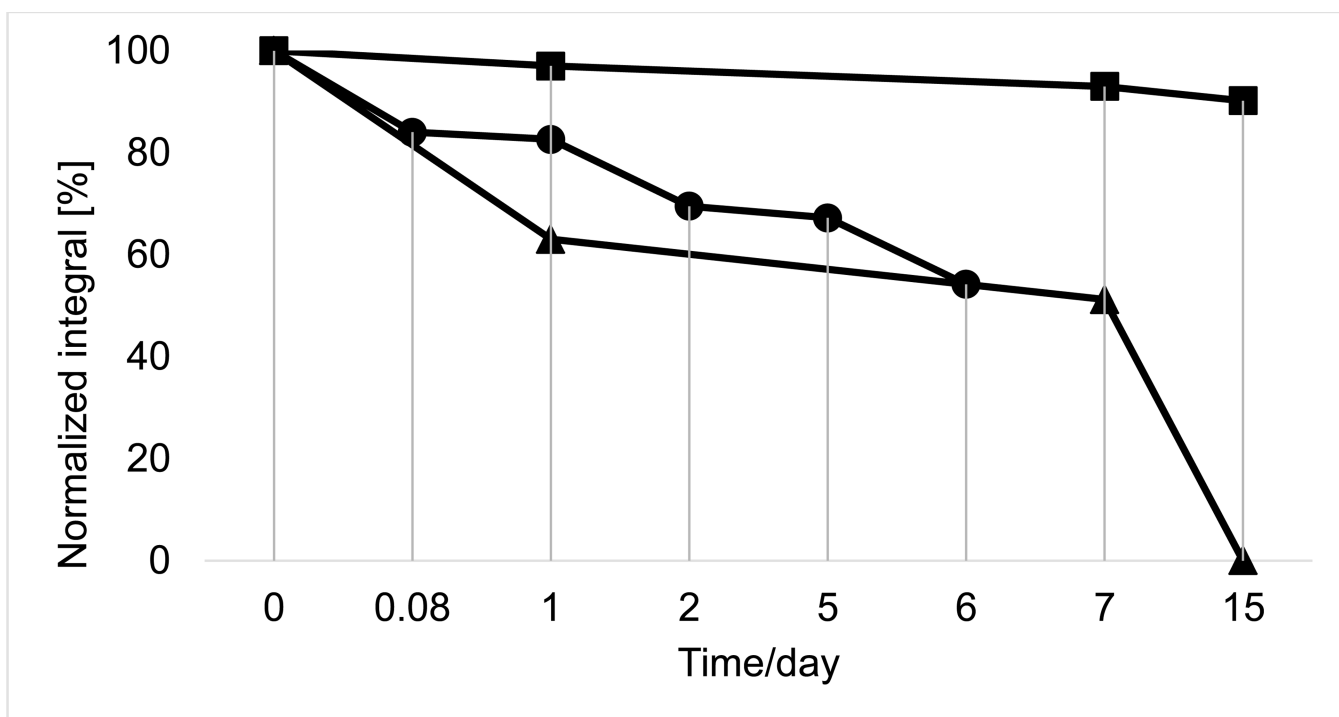


**Figure 3.** Influence of day and UV light on the stability of purified ligustilide (**1**). Stability was assessed in a sealed NMR tube under mass balance conditions for the three samples: tube B1 (exposed to ambient daylight [B1, ▲]), tube kept in the dark [B2, ■]), tube continuously exposed to UV light – 260 nm [B3, ●]), using the 100% qHNMR method.

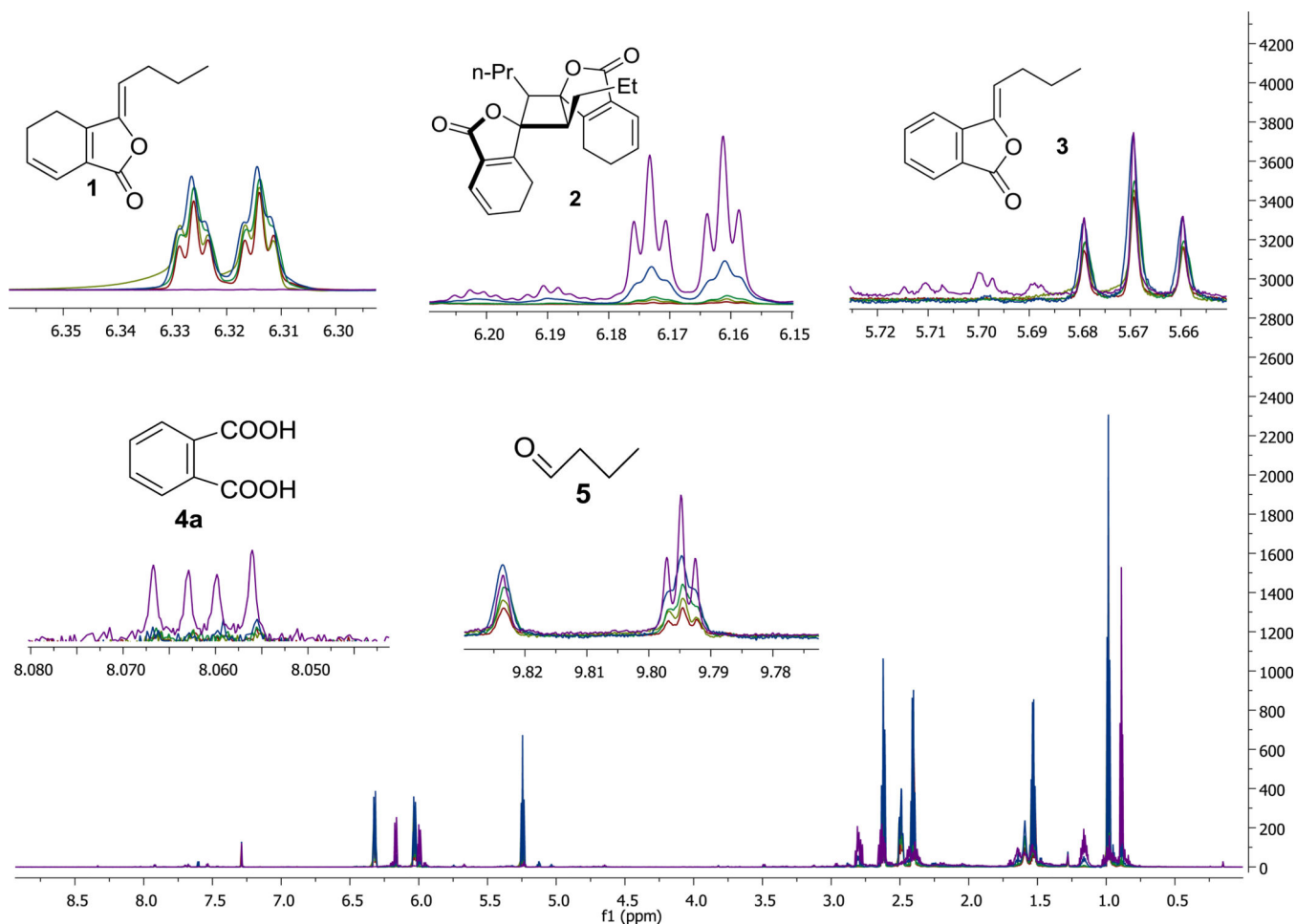


**Figure 4.**

$^1\text{H}$  NMR spectra ( $\text{CDCl}_3$ , 800 MHz) of the degradation products of ligustilide (**1**). The decrease of **1** in sample C1 and concomitant increase of its degradation products was monitored qualitatively and quantitatively by qHNMR. The inserts show characteristic signals of the four main degradation products; **1**: (*Z*)-ligustilide ( $m/z$  190), identified by its characteristic doublet of a triplet signal at  $\delta$  6.317 (1H, 9.6 and 2.1 Hz; H-7), **2**: *endo*-(*Z,Z*)-(3.8',8.3',H-7)-diligustilide ( $m/z$  381), identified by its doublet of a triplet at  $\delta$  6.165 (1H, dt,  $J=9.5$  and 1.9 Hz; H-7), **3**: (*Z*)-butylidenephthalide ( $m/z$  189), showing a triplet at  $\delta$  5.668 (1H, t,  $J=7.8$  Hz; H-8) **4**: phthalic acid anhydride ( $m/z$  148) showed the higher-order resonances of the AA' part of the aromatic AA'XX' spins system at  $\delta$  8.059 (2H, apparent dd with 3.0 and 5.4 Hz line distances, AA'XX' spin analysis yielded  $J=8.2$ , 2.4 Hz), **5**: butyraldehyde, with its characteristic downfield signal at  $\delta$  9.792 (1H, t,  $J=1.8$  Hz). The time-course of the degradation is reflected by the colors: red is day 1, light green day 3, dark green day 14, blue day 30, and violet day 41.

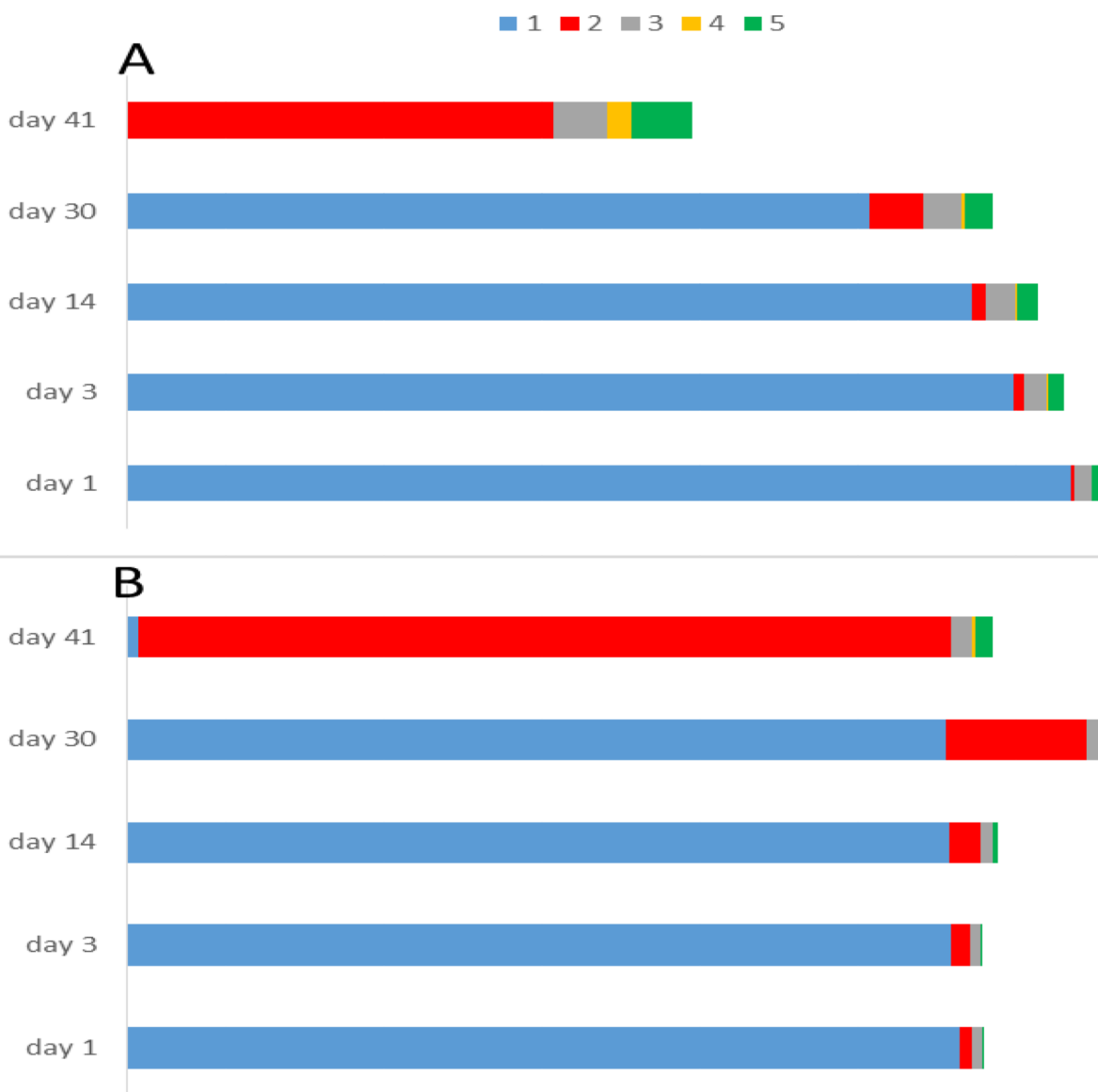


**Figure 5.**

Ligustilide (**1**) degradation in sealed NMR tube in presence (A) and absence of O<sub>2</sub> of Ar (B; Ar degassing). Both samples were kept at  $-20\text{ }^{\circ}\text{C}$  for 30 days, after which the samples were maintained at ambient temperature and in the presence of daylight for the next 10 d.

Comparing the initial TS/RS value of **1** versus those the four main degradation products, was monitored the percentage of their formation in the given conditions. **1**: *Z*-ligustilide, **2**: *endo-Z,Z*-(3.8',8.3', H-7)-diligustilide, **3**: *Z*-butylidenephthalide, **4**: phthalic acid anhydride, **5**: butyraldehyde.



CO<sub>2</sub> Supercritical Fluid Extraction of *Angelica sinensis* Essential Oil (EO): Comparison Between the Standard and Solvent-modified Method.

**Table 1.**

method	extract temperature	vessel temperature	pressure	static extract time	flow rate	modifier	EO yield
standard	50 °C	120 °C	250 psi	20 min	2 mL/min	none	10.0%
modified	50 °C	120 °C	220 psi	30 min	0.5 mL/min	5% MeOH	14.8%